Biophysical Journal
Article

Biophysical Society

Phosphatidylserine Asymmetry Promotes the Membrane Insertion of a Transmembrane Helix

Haden L. Scott,[1] Frederick A. Heberle,[2,4] John Katsaras,[3,4,5,6] and Francisco N. Barrera[1,*]
[1]Department of Biochemistry & Cellular and Molecular Biology, [2]The Bredesen Center for Interdisciplinary Research and Graduate Education, and [3]Department of Physics and Astronomy, University of Tennessee, Knoxville, Tennessee; [4]Shull Wollan Center—a Joint Institute for Neutron Sciences and [5]Large Scale Structures Group, Neutron Sciences Directorate, Oak Ridge National Laboratory, Oak Ridge, Tennessee; and [6]Department of Physics, Brock University, St. Catharines, Ontario, Canada

ABSTRACT The plasma membrane (PM) contains an asymmetric distribution of lipids between the inner and outer bilayer leaflets. A lipid of special interest in eukaryotic membranes is the negatively charged phosphatidylserine (PS). In healthy cells, PS is actively sequestered to the inner leaflet of the PM, but PS redistributes to the outer leaflet when the cell is damaged or at the onset of apoptosis. However, the influence of PS asymmetry on membrane protein structure and folding are poorly understood. The pH low insertion peptide (pHLIP) adsorbs to the membrane surface at a neutral pH, but it inserts into the membrane at an acidic pH. We have previously observed that in symmetric vesicles, PS affects the membrane insertion of pHLIP by lowering the pH midpoint of insertion. Here, we studied the effect of PS asymmetry on the membrane interaction of pHLIP. We developed a modified protocol to create asymmetric vesicles containing PS and employed Annexin V labeled with an Alexa Fluor 568 fluorophore as a new probe to quantify PS asymmetry. We observed that the membrane insertion of pHLIP was promoted by the asymmetric distribution of negatively charged PS, which causes a surface charge difference between bilayer leaflets. Our results indicate that lipid asymmetry can modulate the formation of an α-helix on the membrane. A corollary is that model studies using symmetric bilayers to mimic the PM may fail to capture important aspects of protein-membrane interactions.

INTRODUCTION

The mammalian plasma membrane (PM) is a highly complex structure composed of hundreds of different lipids. Moreover, it has long been established that these lipids are not randomly arranged in the bilayer but instead are asymmetrically distributed between the two bilayer leaflets (1). Specifically, the outer leaflet is enriched in phosphatidylcholines (PCs) and sphingomyelins, whereas the amino-containing glycerophospholipids such as phosphatidylserine (PS) and phosphatidylethanolamine (PE) are primarily located in the inner leaflet (1–4). Lipid asymmetry is entropically unfavorable and must be actively maintained by the cell. Two classes of ATP-dependent transporters, with the ability to move phospholipids unidirectionally to a given leaflet (5–8), have evolved for this purpose. These enzymes, termed flippases and floppases, counteract the movement of lipids down their concentration gradients by active translocation. Additionally, lipid scrambling occurs through the non-ATP-dependent activation of the scramblase transporter (6,9,10). Although there is still considerable uncertainty regarding the physiological role of PM asymmetry, its importance for proper cellular function is clear (9).

The maintenance of proper PS asymmetry is important for cellular viability (9). The presence of the negatively charged PS in the inner leaflet enhances the binding of many cytosolic proteins, including key signaling proteins such as phospholipase C or KRAS (11,12). Unsurprisingly, the loss of PS asymmetry is correlated with cellular malfunction and even death. For example, cell damage can result in the activation of scramblases, promiscuous lipid transporters that rapidly destroy membrane asymmetry (13). The resulting exposure of PS on the outer leaflet is a recognition signal for apoptosis to proceed via the binding of annexins on the surface of macrophages (9).

Membrane proteins are fundamental membrane constituents that constitute roughly half its mass (14,15). Transmembrane (TM) proteins contain sequences consisting largely of hydrophobic amino acids, driving protein insertion into the hydrophobic core of the membrane (16). Membrane proteins use the continuous ribosome-translocon

Submitted November 28, 2018, and accepted for publication March 6, 2019.

*Correspondence: fbarrera@utk.edu

Frederick A. Heberle's present address is Department of Integrative Biology and Pharmacology, University of Texas Health Science Center, Houston, Texas.

Editor: Charles Deber.

https://doi.org/10.1016/j.bpj.2019.03.003

channel to enter the membrane. TM helices, but not soluble ones, can fold cotranslationally inside the ribosome tunnel (17). Similarly, the helix formation in pHLIP occurs before membrane insertion, which results in the translocation of the C-terminal end (18,19). However, how lipid composition affects TM helix insertion is poorly known (20).

A recent study investigated the importance of the lipid environment using the bacterial protein lactose permease (LacY) (21) and instead of using a recently developed method to create lipid asymmetry in freely floating model membranes (22). The authors found that PE asymmetry led to topological reorientations of LacY. However, the experimental system was far from ideal because LacY dissipated bilayer asymmetry by strongly increasing the rate of lipid flip-flop (21). That membrane asymmetry can influence the topological orientation of membrane proteins is worthy of further study. PM proteins are synthesized in the symmetric membrane of the endoplasmic reticulum (ER), yet their final destination is an asymmetric membrane (4,23). It is unknown if the dramatically different ER and lipid environment from the ER to the PM affects membrane proteins that have the potential to change their topology after membrane insertion.

Here, we use the pH low insertion peptide (pHLIP) as a model system to study how PM asymmetry affects the folding and insertion of a TM helix. pHLIP assumes two different membrane topologies depending on the pH as a result of changes in protonation in its seven charged groups. This characteristic enables experimental control of the different topologies of pHLIP, termed State II (membrane associated at a neutral pH) and State III (inserted as a TM helix at an acidic pH) (24,25). Unlike membrane active peptides such as GALA, pHLIP does not lead to membrane leakage or disruption, a requisite for maintaining membrane asymmetry (24,26). pHLIP has been studied in different membrane compositions, and its behavior is well characterized (24,27,28). Using symmetric PS vesicles, our lab previously showed that both the insertion pK and the insertion depth in State II decreased in the presence of symmetric PS (28). We proposed that both observations can be explained by an unfavorable interaction between the negatively charged PS headgroup and the seven negative charges present on pHLIP at a neutral pH (28). However, it is unknown how a more biologically faithful model system, one in which PS is enriched in the inner leaflet, would influence pHLIP insertion. To test this, we modified a technique for producing freely floating vesicles to mimic the asymmetric distribution of PS in the PM (29). We found that PS asymmetry caused an increase in the midpoint of pHLIP insertion, suggesting that a physiologically relevant transbilayer charge distribution—i.e., less negative charge in the outer compared to the inner leaflet—lowers the energetic barrier for insertion. This finding proposes a general role for PS asymmetry in promoting the folding of TM proteins.

MATERIALS AND METHODS

Materials

The lipids 1-palmitoyl-d31-2-oleoyl-*sn*-glycero-3-phosphocholine (POPCd31), 1-palmitoyl-2-oleoyl-*sn*-glycero-3-phosphocholine (POPC), and 1-palmitoyl-2-oleoyl-*sn*-glycero-3-phospho-L-serine (POPS) were purchased from Avanti Polar Lipids (Alabaster, AL) and used as is. Annexin V, Alexa Fluor 568 conjugate (Annexin V-568), was purchased form Thermo Fisher Scientific (Waltham, MA) and assayed for concentration with an Agilent Cary 100 Ultraviolet-Visible Spectrophotometer (Agilent Technologies, Santa Clara, CA) using an extinction coefficient of 23,380 $M^{-1}cm^{-1}$. pHLIP (sequence: N_t-AAEQNPIYWARYADWLFTTPLLLLDLALLVDA DEGTCG-C_t), synthesized using standard solid phase protocols and purified by reverse-phase high performance liquid chromatography to greater than 95% purity, was purchased from P3 BioSystems (Louisville, KY). A lyophilized pHLIP stock was dissolved in buffer (10 mM NaP_i (pH 8.0)) and assayed for concentration by ultraviolet-visible using an extinction coefficient of 13,940 M^{-1} cm^{-1}. Methyl-β-cyclodextrin (mβCD), sucrose, 4-(2-hydroxyethyl)-1-piperazineethanesulfonic acid) (HEPES), 2-(*N*-morpholino) ethanesulfonic acid (MES), calcium chloride ($CaCl_2$), sodium acetate (NaOAc) buffer, and sodium phosphate (NaPi) buffer were all purchased from Sigma-Aldrich (St. Louis, MO). Buffers were prepared by weighing the powder and adding ultrapure water to obtain the desired concentration. HEPES, MES, and NaOAc buffers were adjusted to the correct pH using hydrochloric acid or sodium hydroxide. Ultrapure water was obtained from a Millipore Milli-Q Academic (MilliporeSigma, Burlington, MA) source.

Asymmetric vesicle preparation and quantification

Asymmetric vesicles were prepared following the protocol from (29) with minor modifications because of the inclusion of POPS. Briefly, PS asymmetry was generated by using mβCD to catalyze the exchange of POPCd31 from multilamellar vesicles (MLVs) to the outer leaflet of large unilamellar vesicles (LUVs) composed of POPCd31 and POPS in a molar ratio of 93/7. Lipid films for donor MLVs were hydrated with 0.75 mL of 20% w/w sucrose, and films for acceptor vesicles were hydrated with 0.5 mL ultrapure water; the concentrations of aqueous donor and acceptor were 25.3 and 12.6 mM, respectively. Donors were subjected to 4× freeze/thaw cycles, whereas acceptors went through 5× cycles. Donor MLVs were diluted to 4.38 mM and incubated with 4.33 mL of 35 mM mβCD for 2 h at room temperature in an 8:1 molar ratio. The acceptors were extruded through a 100 nm pore size polycarbonate membrane (31 passes) using a Mini Extruder (Avanti Polar Lipids) to form LUV*s*. Acceptor LUVs were then added to the donor/mβCD mixture and incubated for 1 h at 30°C (although the original protocol calls for incubation at room temperature, we found that a slightly increased temperature allowed for greater PS exchange). The donor:acceptor molar ratio during exchange was 3:1. After the exchange step, residual MLVs were removed by centrifugation at 20,000 × *g* for 1 h, and the supernatant containing the asymmetric vesicles was washed four times with buffer (1 mM HEPES/1 mM $CaCl_2$ (pH 7.4)) and concentrated using a 100,000 molecular weight cut-off centrifugal filter device (Amicon Ultra-15; EMD Millipore, Billerica, MA). Gas chromatography coupled to mass spectrometry (GC/MS) (7890A; Agilent Technologies) was used to quantify the initial and final POPS concentrations in the vesicles after the derivatization of the lipids to fatty acid methyl esters as in (29). The fatty acid methyl esters derived from protiated and deuterated palmitic acid were separately resolved by GC (30), allowing for the quantitation of the mole fractions of POPCd31 and POPS (29). Three replicate samples of the initial acceptor vesicles and of the final asymmetric vesicles were measured to determine error bars. The molar percentage of POPS in the outer leaflet was calculated using the equation:

$$V_T C_T = C_A V_A + C_B V_B, \quad (1)$$

where V_T is the total fractional vesicle volume (1), C_T is the total concentration of POPS, C_A and C_B are the concentrations of POPS in the outer and inner leaflet, and V_A and V_B are the volume fractions of the outer and inner leaflet (0.51 and 0.49, respectively, for 100-nm diameter vesicles). Vesicle concentration was determined by an inorganic phosphate assay (31). Dynamic light scattering (DLS) was used to determine the size and polydispersity of both the acceptors and asymmetric vesicles using either a Brookhaven Instruments BI-200SM (Brookhaven Instruments, Holtsville, NY) or a Wyatt DynaPro NanoStar (Wyatt Technology, Santa Barbara, CA) instrument. For the Wyatt instrument, the MW-R model was set for globular proteins, and the Rg model was set for spheres. For the Brookhaven Instrument, 90° light scattering was measured using a 633-nm HeNe laser light source operated at 30 mW and a detector aperture of 200 μm. Data collection time was 4 min, and the obtained autocorrelation curve was fit with both CONTIN and cumulant analyses. DLS measurements were taken at 25°C.

Annexin V assay and lipid flip-flop

Symmetric POPC vesicles with 0, 1, 2.5, 3.5, 5, 8, 10, 15, 20, and 50 mol % POPS were prepared in buffer (1 mM HEPES/1 mM $CaCl_2$ (pH 7.4)) as described above. Annexin V-568 (stock concentration determined via UV/Vis) and buffer (25 mM NaOAc/1 mM $CaCl_2$ (pH 5.4)) were added to the vesicles and incubated in the dark for 1 h; the final lipid and Annexin V-568 concentrations were 50 μM and 0.52 μM, respectively, and the final sample pH was 5.5. Fluorescence measurements were made at room temperature with a Photon Technology International (Edison, NJ) QuantaMaster fluorometer using the following instrument settings: excitation wavelength 579 nm, emission wavelength 601 nm, 15 s integration, 90° excitation polarization, 0° emission polarization, and 4.8 nm excitation and emission slit widths. Appropriate lipid blanks were subtracted in all cases, and changes in intensity were normalized to the POPC control. Symmetric samples of varying POPS concentrations were used to determine a calibration curve that was fitted with the equation:

$$Signal = F_0 + \Delta F(K_p x)/(55.3 + K_p x), \quad (2)$$

where F_0 is the initial fluorescence intensity, ΔF is the change in fluorescence intensity, x is the molar percentage of POPS, and 55.3 is the molar concentration of water (32,33). This equation was used to determine the molar partition coefficient, K_p, of Annexin V binding to the membrane in the presence of different levels of PS. Using this assay, we determined the molar percentage of POPS exposed at the outer leaflet of the asymmetric LUVs (aLUVs) via a decrease in Annexin V-568 intensity as it bound PS. Using Annexin V-568 intensity values in the presence of asymmetric samples, we normalized the values to the PC control and inputted them into Eq. 2 to determine the molar percentage of POPS in the outer leaflet. Measurements on asymmetric samples were taken for multiple days to assess the level of asymmetry and lipid flip-flop.

Lipid flip-flop in the presence of pHLIP was determined by performing the Annexin assay with aLUV*s*. pHLIP was incubated with POPC (control) and aLUVs for 1 h at pH 7.4. Annexin V-568 was then added and incubated as described earlier. The final pH was 5.5, and the final pHLIP concentration was 0.25 μM. Intensity changes in the presence of pHLIP were analyzed as described earlier.

Calculation of leaflet surface potential

The surface potential of each leaflet in the asymmetric bilayer was calculated using the Grahame equation,

$$\sigma = \sqrt{8 c_0 \varepsilon \varepsilon_0 k_B T} \sinh\left(\frac{e\psi_0}{2k_B T}\right), \quad (3)$$

where σ is the surface charge density, c_0 is the ion concentration, ε is the dielectric constant (here, 78.3), ε_0 is the vacuum permittivity, k_B is the Boltzmann constant, T is the absolute temperature (here, 298.2 K), and ψ_0 is the surface potential (34). The surface charge density was calculated using the Gouy-Chapman Theory (34) separately for each leaflet using the measured POPS concentrations, and assuming an average area per lipid of 62.7 $Å^2$ (35). Solving Eq. 3 for ψ_0 gives the surface potential.

Intrinsic tryptophan fluorescence spectroscopy

Symmetric POPCd31 vesicles with 0, 3, 7, and 30 mol% POPS were prepared via extrusion using a 100-nm pore size membrane (Whatman, Maidstone, UK) using a Mini Extruder (Avanti Polar Lipids) in 10 mM NaP_i (pH 8) to form LUV*s*. aLUVs were in 1 mM HEPES/1 mM $CaCl_2$ (pH 7.4). Both symmetric and asymmetric vesicles were incubated with pHLIP for 1 h at room temperature for a final lipid:peptide molar ratio of 200:1. Final peptide concentration was 1 μM. It was previously shown that the inclusion of the C-terminal cysteine in pHLIP does not cause disulfide-mediated dimerization (36). A pH titration was performed by adjusting the pH of the different samples with 100 mM stocks of NaOAc, MES, or HEPES buffers (25 μL) to obtain the desired final pH values. The final sample volume was 140 μL for symmetric samples and 125 μL for asymmetric samples. A 2.5-mm bulb pH electrode (Microelectrodes, Bedford, NH) was employed to measure the final pH of each sample. Emission spectra were recorded using a Photon Technology International QuantaMaster fluorometer at room temperature with the following settings: excitation wavelength 280 nm, emission wavelength range 310–400 nm, and excitation and emission slits 3 nm. Appropriate lipid blanks were subtracted in all cases. Data were analyzed by calculating the spectral center of mass (CM) with the following equation:

$$CM = \sum_i I_i \lambda_i \Big/ \sum_i I_i, \quad (4)$$

where Ii is the fluorescence intensity at wavelength λi. CM uses the entire spectral range of the data to inform on the local environment of the two tryptophan (Trp) residues (37,38). The data were also analyzed by monitoring changes in the fluorescence emission intensity FI at 335 nm, which is directly proportional to the population of molecular species present (39). CM and FI pH titrations were then fitted to determine the pK using the equation:

$$Signal = \left(F_a + F_b 10^{m(pH-pK)}\right)/\left(1 + 10^{m(pH-pK)}\right), \quad (5)$$

where *Fa* is the acidic baseline, *Fb* is the basic baseline, m is the slope of the transition, pK is the midpoint of the curve, and *Signal* refers to the changes in the fluorescence or CD signals as a function of pH.

Circular dichroism

CD measurements were performed using a Jasco (Easton, MD) J-815 Spectropolarimeter at 25°C. pHLIP was incubated with POPC, symmetric POPC/POPS 97/3, or asymmetric vesicles (prepared as described earlier) in 10 mM NaP_i buffer (pH 8.0) for 1 h. The pH was then adjusted with 100 mM NaOAc or NaP_i to a range of the desired final pH values. The final sample volume, in each case, was 250 μL. For POPC samples, the lipid:peptide molar ratio was 200:1 with a final peptide concentration of 7 μM and a final lipid concentration of 1.4 mM. For the POPC/POPS 97/3 and asymmetric samples, the final peptide concentration was 3 μM, and the final lipid concentration was 600 μM. The helical content changes of pHLIP were

determined by measuring the ellipticity at 222 nm as a function of pH as in (18). Molar ellipticity was determined with the following equation:

$$[\theta] = \theta/(10lc(N-1)), \quad (6)$$

where Θ is the measured ellipticity, l is the cell path length, c is the protein concentration, and N is the number of amino acids (here, 38) (40). Calculated molar ellipticity at 222 nm was plotted against the measured pH, and the resulting sigmoidal transition was fitted using Eq. 2 to obtain the pK_{CD}. Spectra were collected from 260 to 195 nm for samples at pH 8 and 4 using the same temperature and scan rate as earlier but with a 1 nm step size. Spectra were collected to check for secondary structure other than at 222 nm, which allowed for a detailed comparison of pHLIP in symmetric and asymmetric membranes.

Statistical analysis

Statistical analysis was performed on the pK values and samples from the Annexin assay to determine if the observed changes were significant. The analysis was performed using SPSS v25 software (IBM Analytics, Armonk, NY). One-way ANOVA and two different post hoc multiple comparisons tests were used based on the homoscedasticity (two-sided Dunnett t-test) or heteroscedasticity (Dunnett T3) of the data. Both the two-sided Dunnett t-test and the Dunnett T3 set one variable as the control to compare to all other treatment groups. A two-sided Dunnett t-test was used to determine the statistical significance of pK values determined via Trp fluorescence and CD by comparing all samples to the asymmetric vesicles sample. A one-way ANOVA was used to determine the statistical significance of the Annexin assay results (Fig. S1). A Dunnett T3 test was used to determine the statistical significance of the stability of POPS asymmetry by comparing day 1 after the exchange to all subsequent days. A two-sided Dunnett t-test was used to determine the statistical significance of lipid flip-flop in the presence of pHLIP by comparing the samples in the presence of pHLIP to samples without pHLIP. $p < 0.05$ was considered significant for all tests.

RESULTS

Preparation and quantification of asymmetric PS vesicles

The goal of this study was to understand how PS asymmetry influences the folding and insertion of a TM helix in a well-controlled and characterized model membrane system. A wide variety of techniques have been developed for the preparation of asymmetric bilayers, each with strengths and weaknesses (41,42). For our study, it was important to use freely floating vesicles rather than solid supported bilayers and to avoid the use of osmolytes that can potentially interact with the bilayer and/or create membrane tension (22,43). To this end, we used the technique of mβCD-mediated lipid exchange pioneered by the London group (22) with modifications that eliminate the requirement for concentrated sucrose in the vesicle core (Fig. 1) (29). Our strategy was to prepare symmetric POPC/POPS acceptor vesicles with PS as a minor component (~7 mol%) and then replace the POPS in the outer leaflet with POPC from a donor vesicle pool to generate asymmetric unilamellar vesicles (aLUVs) with PS enriched in the inner leaflet.

To monitor PS asymmetry, we first used GC/MS to determine the total PS concentration in the aLUVs (29). This required us to use a partially deuterated neutral lipid (POPCd31), which allows the discrimination of fatty acids from POPCd31 compared to the protiated fatty acids from POPS. GC/MS can additionally be used to quantify asymmetry, assuming that PS levels in the inner leaflet are constant (29,30). To directly determine the amount of PS exposed in the outer leaflet, we employed externally added Annexin V-568. Annexin V specifically binds to PS headgroups in the presence of calcium (44) and is routinely used in cell biology for the determination of the onset of apoptosis, which is marked by the exposure of PS to the extracellular environment (45). In symmetric vesicles, we observed a hyperbolic decrease in the fluorescence intensity of Annexin V-568 as PS concentration was increased (Fig. 2). Using these data as a calibration curve, we then assayed the concentration of exposed PS in aLUV*s*. Before outer leaflet exchange, the acceptor LUVs had an average exposed PS concentration of ~7 mol% ($n = 5$), which decreased to ~3 mol% in the aLUVs (Fig. S1). Statistical analysis revealed no significant differences in the exposed PS concentration among the aLUV exchanges ($p > 0.05$), an indication that the preparation of asymmetric PS-containing vesicles was robust and reproducible. After we had established the agreement between GC/MS and the

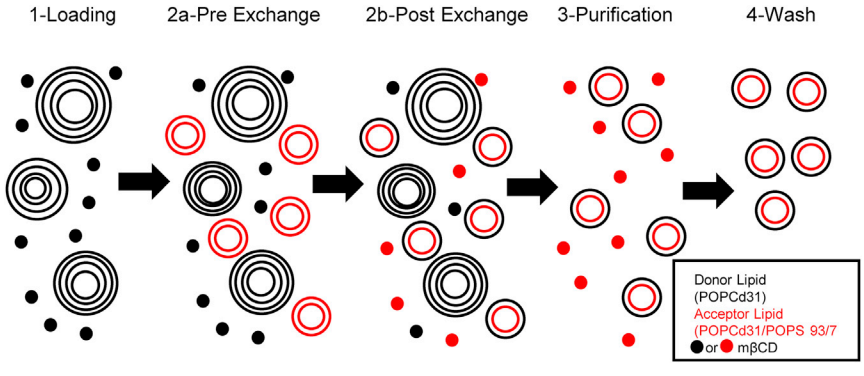

FIGURE 1 Cyclodextrin-mediated exchange used to generate asymmetric vesicles. Steps were as follows: *1*- mβCD is incubated with sucrose-loaded donor multilamellar vesicles to load donor lipid into mβCD. *2a*- Acceptor unilamellar vesicles are added for exchange to proceed with mβCD delivering donor lipid (*black*) to the acceptors. *2b*- Post delivery of donor lipid to acceptor vesicles yield asymmetric vesicles and mβCD loaded with donor (*black*) and acceptor (*red*) lipid. *3*- Donors are removed by centrifugation. *4*- Asymmetric vesicles are washed in buffer of interest to remove mβCD. Black mβCD corresponds to the POPCd31-loaded state, and red mβCD is the loaded form containing POPS. Adapted from (29,30). To see this figure in color, go online.

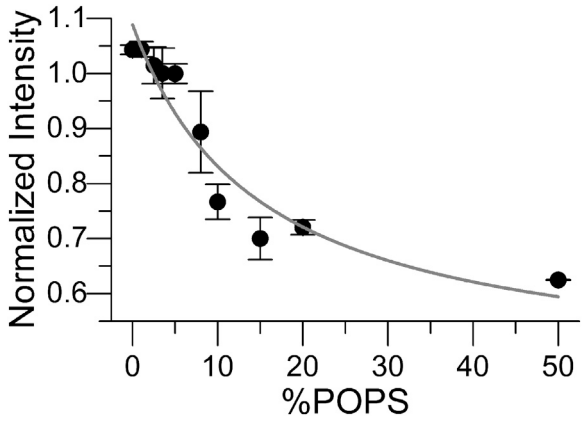

FIGURE 2 Annexin V-568 used to quantify the amount of PS in the outer bilayer leaflet. In the presence of PS, fluorescent Annexin V-568 exhibits a decreased intensity with an increasing concentration of exposed (outer leaflet) PS. Symmetric PC vesicles containing various levels of PS were used to generate a calibration curve. The line is fit to the data using a binding model (Eq. 2). $n = 2$–5. Error bars are SD.

Annexin V assay to measure PS asymmetry, we used the second method in the following experiments.

Next, we investigated the stability of aLUVs by monitoring PS asymmetry over time. aLUVs, once prepared, will gradually equilibrate to a symmetric state via passive lipid flip-flop. Although some studies have reported fast flip-flip (half times of seconds to minutes) in supported bilayers (46), there is a general agreement that lipid flip-flop is much slower (half times of hours to days) in vesicles (47). Fig. 3 A shows that no significant loss of asymmetry in 4-d-old aLUVs occurred ($p > 0.05$). We also examined the influence of pHLIP on the stability of PS asymmetry. It has been previously reported that the presence of TM peptides can accelerate lipid flip-flop and lead to a rapid loss of membrane asymmetry (48–50). However, we found that pHLIP in either State II or III did not lead to a significant loss of PS asymmetry over 3 h via the Annexin assay, a period of time greater than the time needed to complete our fluorescence spectroscopic assay ($p > 0.05$) (Fig. 3 B). We also observed no changes in lipid flip-flop at room temperature over a period of 108 h (data not shown). These results indicate that pHLIP does not influence the rate of POPS flip-flop on our experimental timescales.

PS membrane asymmetry promotes membrane insertion of pHLIP

The membrane insertion of pHLIP occurs in multiple steps as the pH is acidified (51,52), and we recently reported that the insertion process is characterized by at least three macroscopic pK values that require different analyses and/or techniques for determination (18,53). Specifically, when using the fluorescence emission spectra of the two Trp residues to monitor insertion into symmetric POPC vesicles, we found different insertion pK values depending on whether the response metric was the spectral CM or the fluorescence intensity at fixed wavelength (FI) (18). We refer to these insertion pH midpoints as pK_{CM} and pK_{FI}, respectively, and pK_{CM} reports on earlier events in the membrane insertion process than pK_{FI}, as detailed in the Discussion section.

We first used both native Trp and nitrobenzoxadiazole (NBD) conjugated to a C-terminal cysteine residue fluorescence, as described previously (18), to determine pHLIP insertion pKs in symmetric POPCd31/POPS vesicles with an increasing POPS concentration. As previously reported (54), decreasing the solution pH caused a shift in the Trp emission maxima to shorter wavelengths and an increase in intensity (Fig. 4 A). These changes result from alterations in the local environment of the Trp residues, consistent with pHLIP insertion into the membrane. As NBD is also an environmentally sensitive dye (55–59), similar changes were observed compared to Trp (data not shown). We then analyzed the emission spectral changes to determine the insertion pK_{CM}, pK_{FI}, and pK_{NBD} (Fig. 4, B–E; Fig. S2). We observed both pK_{CM} (Fig. 4 D) and pK_{FI} (Fig. 4 E) decreased by ~0.4 units as POPS concentration increased from 0 to 7 mol%. We also found that pK_{FI} was ~0.5 units lower than pK_{CM} at each PS concentration. Similarly, we observed that the pK_{NBD} value was comparable to previous

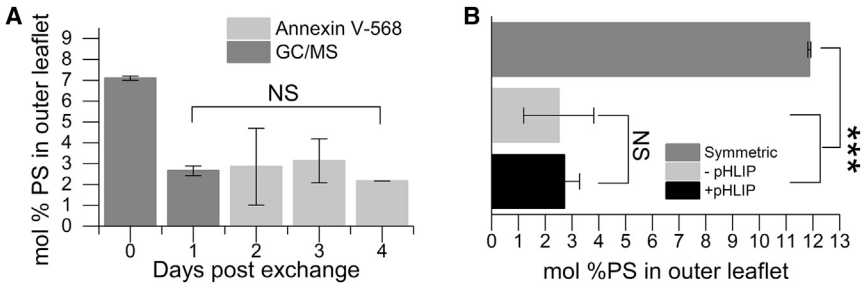

FIGURE 3 PS asymmetry is stable for days post-exchange and in the presence of pHLIP. (*A*) Stability of asymmetric vesicles was monitored for a period of 4 d post exchange. Day zero indicates the level of PS in the outer leaflet before exchange. Days 1–4 display the level of asymmetry post exchange. Both GC/MS and Annexin V-568 were used to determine the level of membrane asymmetry independently. Error bars represent the measurement uncertainty for each day obtained from replicates. (*B*) Shown is a comparison of PS levels in the outer leaflet of asymmetric vesicles incubated in the presence and absence of pHLIP. Here, pHLIP was incubated with asymmetric vesicles in both State II and III within the same sample by changing the pH after a given period of time. The symmetric vesicle PS level is before exchange, and the asymmetric vesicle level is post exchange. Here, the symmetric PS level was ~12%. The inclusion of pHLIP in the asymmetric vesicles does not lead to a loss of membrane asymmetry over a 3-h period post addition of pHLIP. ***$p < 0.005$; NS, no significance. $n = 3$–4. Error bars are SD.

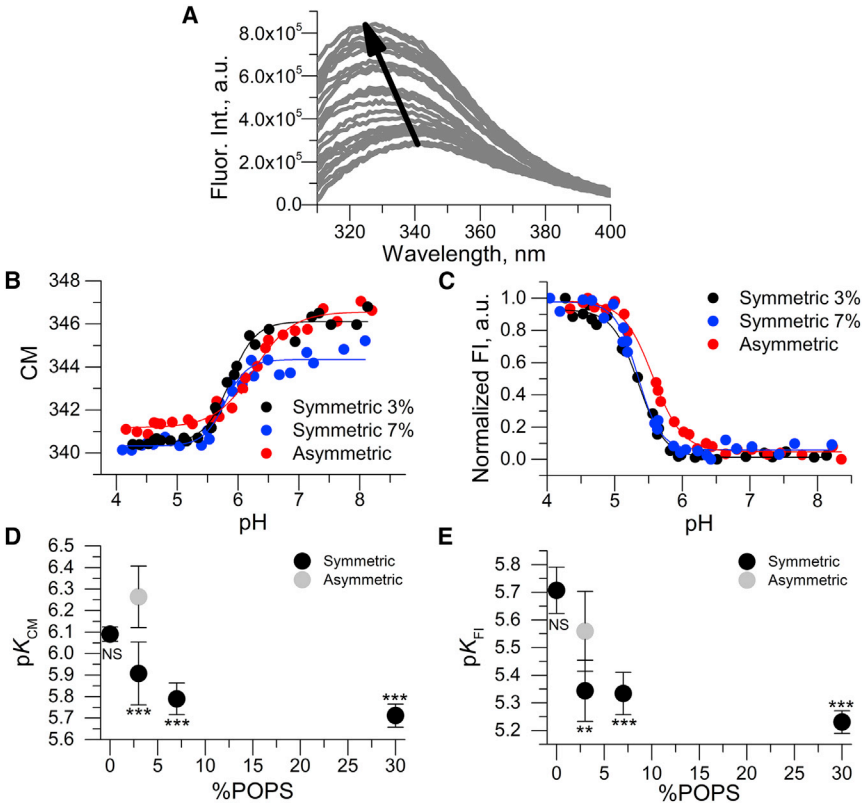

FIGURE 4 PS membrane asymmetry alters pK_{CM} and pK_{FI}. Intrinsic Trp fluorescence indicates that PS membrane asymmetry affects the pK of insertion of pHLIP causing a basic shift in pK values compared to symmetric PS. (*A*) Representative Trp spectra display changes in Trp fluorescence as the pH is decreased (*arrow*) in asymmetric vesicles. (*B*) and (*C*) Shown are representative pK titrations for CM and FI Trp fluorescence analysis comparing asymmetric samples with symmetric samples with 3% and 7% PS. Titrations were fit to Eq. 3 to yield pK_{CM} and pK_{FI}. (*D*) and (*E*) show a comparison of pK of insertion between asymmetric and symmetric vesicles with varying levels of PS for both a CM (*D*) and FI (*E*) analysis. Statistical analysis was conducted comparing asymmetric to symmetric samples (one-way ANOVA, two-sided Dunnett *t*-test). $^{**}p < 0.01$; $^{***}p < 0.005$; NS, no significance. $n = 3$–5 for (*D* and *E*). Error bars are SD. To see this figure in color, go online.

results in symmetric vesicles (18) and decreased in the presence of symmetric PS (Fig. S2). The comparable influence of PS suggests that deuteration does not influence the insertion of pHLIP. However, symmetric membranes do not recapitulate the PM conditions, prompting the study of PS asymmetry.

We next examined aLUVs that typically contained ~3 mol% PS in the outer leaflet and ~7 mol% PS in the inner leaflet. We observed a statistically significant increase in both pK_{CM} and pK_{FI} compared to symmetric membranes with similar PS concentration ($p < 0.05$). Specifically, pK_{CM} of the asymmetric vesicles was 6.26 ± 0.14 compared to 5.91 ± 0.15 and 5.79 ± 0.07 for symmetric vesicles containing 3 and 7 mol% PS, respectively (Fig. 4 D). Similar changes were observed in pK_{FI}—the aLUV value was 5.56 ± 0.14, whereas it was 5.34 ± 0.11 and 5.33 ± 0.08 for symmetric samples containing 3 and 7 mol% PS, respectively (Fig. 4 E). Remarkably, pK_{CM} for the aLUVs was even higher than that of symmetric vesicles lacking PS, with the difference in the two pK values (i.e., pK_{CM}–pK_{FI}) increasing to nearly 0.7 units compared to 0.4–0.55 units for symmetric membranes. For pK_{NBD}, we observed no statistically significant difference in the aLUV samples when compared to symmetric samples containing 3% PS (Fig. S2). The increased pK_{CM} and pK_{FI} suggests that PS asymmetry promotes the membrane insertion of pHLIP in a manner that cannot be simply predicted from the outer leaflet composition.

Secondary structure formation is not altered by PS membrane asymmetry

pHLIP must adopt a helical structure before membrane insertion (33,60). Using circular dichroism (CD), we previously observed that PS has no influence on the helical content of pHLIP in State II or III or in symmetric vesicles composed of POPC/POPS 90/10 mol%. Oriented CD (OCD) performed on supported bilayers also established that pHLIP forms a TM helix in the presence of PS (28). Fig. 5 A shows CD spectra of pHLIP in aLUVs at pH values representing State II (pH 8) and State III (pH 4), revealing that pHLIP exhibits comparable helical content whether the membrane contains an asymmetric or symmetric PS distribution (28). This result suggests that PS asymmetry has little effect on pHLIP secondary structure at the initial and final states of the insertion process. We did not perform OCD experiments because none of our methods could assess membrane asymmetry on the OCD sample. Although we could not directly assess the TM state at an acidic pH, the high similitude in fluorescence and CD results strongly suggest that in asymmetric conditions, pHLIP still can form a TM helix.

As mentioned in the previous section, we recently proposed that different analysis methods for determining the insertion pK report independently on the protonation of different acidic residues in pHLIP (18). Specifically, we found that pK_{CD} informs on the midpoint of helical

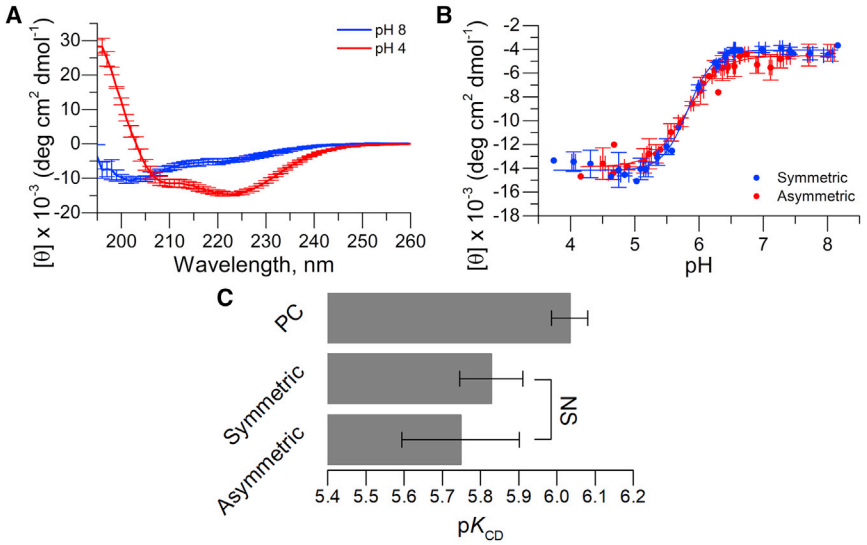

FIGURE 5 PS membrane asymmetry has no substantial influence on the helical formation of pHLIP. (*A*) Average CD spectra of pHLIP in the presence of PS asymmetry is shown. pH 8 and 4 represent the membrane adsorbed and transmembrane states of pHLIP, respectively. (*B*) Average CD titrations comparing symmetric and asymmetric POPC/POPS vesicles with 3% PS in the outer bilayer leaflets for both cases. Lines indicate fits to the data using Eq. 3. Error bars are the SD. (*C*) pK_{CD} was obtained from titrations of PC and symmetric PC/PS with 3% PS and with asymmetric PS samples. No statistical significance (one-way ANOVA) is observed between symmetric and asymmetric PS, suggesting that asymmetric PS does not influence the insertion process of pHLIP as monitored by CD. NS, no significance. n = 3–4. Error bars are SD. To see this figure in color, go online.

formation on the membrane surface. Because pK_{CM} and pK_{FI} showed a significant increase in asymmetric PS vesicles, we investigated if pK_{CD} was similarly affected. Fig. 5 B shows a comparison of average pH titrations of symmetric (3 mol% PS) LUVs and aLUVs containing ~3 mol% PS in the outer leaflet. Fig. 5 C shows no significant effect of PS membrane asymmetry on the pK_{CD} compared to symmetric samples ($p > 0.05$), suggesting that PS asymmetry affects only some steps in the membrane insertion of pHLIP but not the final membrane translocation.

DISCUSSION

PS asymmetric vesicles can be prepared and are stable over multiple days

Membrane lipid asymmetry is a key property of cellular membranes (1). Membrane asymmetry is maintained by ATP-dependent enzymes that translocate lipids to their intended leaflet with a high headgroup specificity, whereas subgroups of the ATP-binding cassette proteins flop lipids with low headgroup specificity (5–8). Loss of these mechanisms of controlled lipid localization is a property of apoptosis and cell death (9). Additionally, Scott syndrome, a bleeding disorder, is associated with the misregulation of membrane asymmetry (61).

Here, we modified a recently developed technique that uses cyclodextrin to create tensionless PC vesicles with an asymmetric chain distribution (29,47). Cyclodextrins are ring-shaped cyclic oligosaccharides with a hydrophilic outer surface (making them soluble in water) and a slightly hydrophobic cavity that is large enough to accommodate a phospholipid chain. The binding of a hydrophobic lipid chain is favorable because of the displacement of unfavorable water/apolar interactions in the cyclodextrin cavity (62). When added to a vesicle suspension, cyclodextrins thus facilitate the transport of an accessible (i.e., outer leaflet) lipid between vesicles. In this study, we aimed to create vesicles with an asymmetric PS distribution mimicking that found in the mammalian PM. We found that minor variations had to be made to the original technique to accommodate the movement of PS, possibly because of the differences in how mβCD solubilizes PS compared to PC (63). Once the vesicles were prepared, we needed to measure the level of PS asymmetry. A variety of techniques have been described for measuring the asymmetry of different lipid species. We first settled on nuclear magnetic resonance as used by Heberle et al. for determining PC asymmetry (29). However, this approach failed, possibly because of a strong interaction between the positively charged chemical shift reagent Pr^{3+} and the negatively charged PS headgroup (data not shown). We also explored using trinitrobenzenesulfonic acid, a molecule known to interact with PE and PS (64). Unfortunately, trinitrobenzenesulfonic acid showed little sensitivity to PS and failed to accurately detect PS levels in symmetric vesicles (data not shown).

After exhausting the available options from the literature, we took advantage of the well-known PS binding properties of Annexin V (44,45), turning to a fluorescent version of this protein. We observed that the fluorescence intensity of the Annexin V-568 conjugate was sensitive to the concentration of PS in the outer leaflet, which allowed us to assay for PS concentration in asymmetric vesicles using a calibration curve prepared from symmetric vesicles (Fig. 2). We speculate the decrease in Alexa Fluor 568 fluorescence intensity is because of quenching caused by amino acids, like Trp, present in Annexin V (65). Using this assay, together with GC/MS, we were able to consistently quantify the level of PS asymmetry in our aLUV*s*. The Annexin assay showed that PS asymmetry could be generated and was stable for multiple days (Figs. 2 and 3 A). Using this same assay, we also determined that pHLIP did not disrupt asymmetry

(Fig. 3 B). This finding is of fundamental importance because proteins and peptides often cause a loss of lipid bilayer asymmetry (21,48), impeding studies on the effect of lipid asymmetry.

PS asymmetry may be particularly stable in part because of the unfavorable free energy barrier for transporting a negatively charged headgroup across the apolar membrane core. Moreover, pHLIP, with its many negative charges in State II, interacts adversely with PS (28). In State III, pHLIP does not disrupt the membrane and only interacts with a few lipid shells in close proximity to it (24,66). This could explain our observation that pHLIP does not increase the rate of PS flip-flop.

PS asymmetry influences the membrane insertion of pHLIP

The interaction of pHLIP with bilayers depends on the specific lipid composition. However, all previous studies were carried out with symmetric bilayers (27,28,54,67). We have reported that symmetric PS vesicles decreased the insertion pK compared to PC vesicles, with a saturation at ~5 mol% PS (28). This was proposed to result from the unfavorable interaction between the negative charge on the PS headgroup and the seven negative charges on pHLIP at a neutral pH (28). In a similar report, symmetric vesicles containing an assortment of lipid headgroups, including PS, were also found to influence the insertion of pHLIP (67). However, an asymmetric distribution of PS, mimicking the PM, was missing from all these studies.

Here, we study the effect of PS asymmetry on the membrane insertion of pHLIP. However, the membrane insertion of pHLIP is not fully described by one insertion pK, but several pKs have been reported using different analysis methods (18). Specifically, in symmetric PC bilayers, pK_{CM} and pK_{CD} reported on the same pHLIP protonation event(s), whereas pK_{FI} reported on a different one occurring at a lower pH (18). Fig. 4 shows that in PS aLUVs, there is a significant increase in the pK determined from Trp fluorescence using both a CM and FI analysis ($p < 0.05$) compared to a similar symmetric distribution of PS. PS asymmetry thus promotes those protonation events because lower proton concentrations are required.

However, pK_{CD}, which describes the midpoint of helical formation (18), was unaffected ($p > 0.05$) (Fig. 5). Furthermore, we also determined that the pK_{NBD} (pK of translocation) was not influenced by PS membrane asymmetry compared to symmetric membranes with 3% PS. It should be noted that in the whole pH range used for determining the pKs, the PS headgroup remains deprotonated (68,69). No changes in pK_{CD} or pK_{NBD} may indicate that PS asymmetry promotes the burial of Trp residues into the membrane before helical formation is complete and that it does not influence the translocation of the C-terminus across the membrane (Fig. 6). As seen in Figs. 4 and 5, the titration reported by CM is largely complete before a large change occurs in the titration reported by CD, which indicates that in aLUVs, CM and CD are decoupled in reporting the protonation of acidic residues (Fig. 6) (18). The decoupling of CM and CD suggests that PS asymmetry might change the pK_a of D25 and D33 of pHLIP. Decoupling is not observed in samples containing symmetric PC or PS, indicating that early protonations reported by CM are occurring before pHLIP begins to adopt its secondary structure in aLUV*s*. Equally important, the titration reported by FI only started at the point where the CM titration is ending (Fig. 4), suggesting that CM and FI, as in symmetric POPC membranes, are also reporting on different protonation steps in the insertion process (18). Together, the data indicate that PS asymmetry may facilitate the protonations

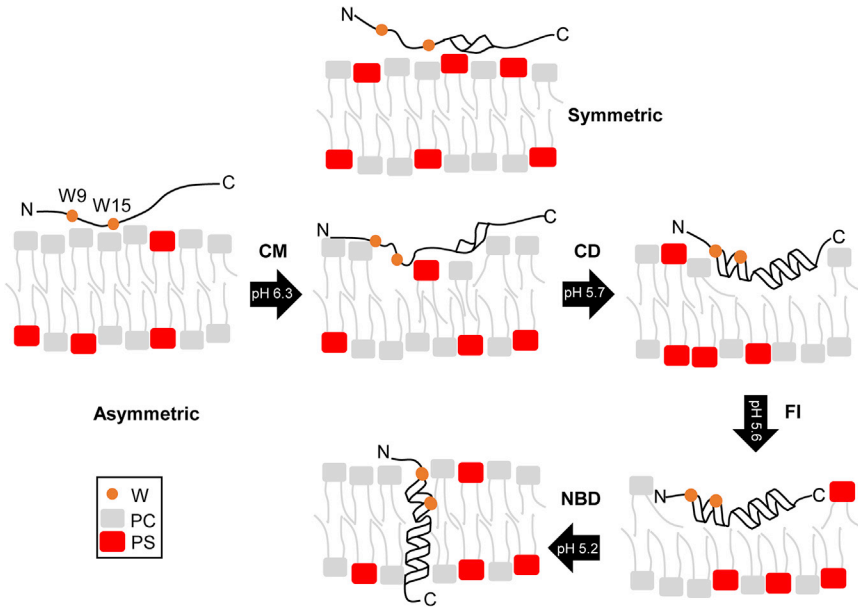

FIGURE 6 Model with the proposed influence of PS membrane asymmetry on the insertion of pHLIP. Black arrows are the transitions between each step in the insertion process, with the corresponding pK values (CM refers to center of mass, FI to Trp fluorescence intensity, and NBD to the fluorescence intensity changes of this dye). Three transitions are represented by their insertion pK. The first transition represents the pK determined by CM. This transition is where the observed influences of membrane asymmetry are most prominent. Comparing to symmetric PS (directly above), the N-terminal region, including the two Trp residues, is more deeply buried in the membrane in the presence of membrane asymmetry. No changes were observed in helical formation or the translocation of the C-terminus, where the NBD moiety is present. To see this figure in color, go online.

of D14, 25, 31, and 33 as protonations of these residues are reported by CM and FI (18).

Changes in membrane electrostatics alter pHLIP insertion

An asymmetric distribution of PS across the two leaflets is expected to change the electrostatics of the membrane (70–72). Lipid bilayers have three distinct potentials, namely the surface, TM, and the dipole potentials (71). The surface potential is created by a buildup of charge on the membrane surface, which propagates out from the membrane and into the aqueous solution. A concentration gradient of ions between the two aqueous solutions bathing the bilayer causes the TM potential. Finally, the dipole potential is a positive potential centered in the hydrophobic core of the membrane, which arises from permanent dipoles in the lipid molecules (71). The observed increases in pK_{CM} and pK_{FI} could be caused by a change in one of these potentials (70–72). For example, an asymmetric distribution of negatively charged lipids should create a surface potential difference across the membrane (70,72,73). As a result, an additional TM potential could potentially arise because of the asymmetric charge distribution from the PS headgroup. The membrane surface potential for each leaflet can be calculated using the Gouy-Chapman model and the Grahame equation (Eq. 3) (34,74). Although our protocol for creating PS asymmetry yielded only a small PS difference of ~4 mol%, this translates into a ~+30 mV difference in surface potential across the membrane, with a less negative exterior. We propose that this surface potential difference might attract the negatively charged aspartic acid (Asp) and glutamic acid (Glu) side chains in pHLIP, leading to the peptide residing deeper in the interfacial region (70). Because of the higher dielectric constant and reduced hydration at this deeper location, the pK_a values of these residues would be expected to increase (75). In contrast, pK_{CD} was not affected by PS asymmetry (Fig. 6), suggesting that asymmetry-induced changes in the surface potential difference do not affect the helical content of pHLIP (33), despite influencing its location at the membrane surface. Some caution with this interpretation is warranted because surface potential differences may not be the only factor driving the observed pK shift. We cannot rule out that lipid asymmetry affects the lipid dipoles in a manner that alters the membrane dipole potential and thus influences the insertion pK of pHLIP (76,77).

pHLIP as a model for the influence of asymmetry on marginally hydrophobic TM domains

TM domains are primarily composed of hydrophobic amino acids, which anchor the domain into the bilayer. However, polar amino acids are commonly found in TM domains and, indeed, Asp and Glu represent ~5% of the residues in TM sequences (16,78). Typically, these polar residues are functionally important, such as in bacteriorhodopsin, in which D85 and D96 (corresponding to D14 and D25 in pHLIP) mediate proton transfer across the membrane (79). A second example is the mammalian sodium/hydrogen exchanger NHE1, in which conserved Asp residues located within the membrane environment allow this exchanger to control the internal pH of the cell (80).

A more accurate amino acid sequence predictor of TM propensity discovered overlap between sequences that were both non-TM and TM (81). These sequences are termed marginally hydrophobic TM domains (mTMD) (82). mTMDs occur in membrane proteins and are unique in that they can assume two different topologies. These involve either the movement of helices in and out of the bilayer or the reorientation of helices within the bilayer after insertion (83–85). This orientation change is a direct consequence of the presence of polar residues, including Asp and Glu, which reduce their hydrophobicity compared to standard TM domains (83–85). Some examples of proteins that have shown dual topology and mTMDs are the human aquaporin water channel APQ1, the hepadnaviral large envelope protein, and the ATP-gated ion channel subunit P2X2 (along with the related ASIC protein) (86–88).

Like mTMDs, pHLIP can adopt two different membrane topologies because of the presence of its polar residues. In the case of pHLIP, the topological change can be easily measured in reconstituted systems because TM insertion is triggered by a mere drop in pH. We propose that pHLIP might be used as a model system to gain mechanistic insights into topological transitions in membranes and speculate that membrane asymmetry might influence the membrane location of other peptides and proteins. Specifically, mTMD could experience topological transitions when exposed to membrane asymmetry changes, particularly those containing amino acids with charged side chains.

TM proteins are synthesized at the membrane of the ER and are transported to the PM via the Golgi apparatus. Membrane proteins experience environmental changes during this transit. Specifically, there is a difference in environmental pH because the lumen of the Golgi is acidic, whereas the ER lumen and the cytoplasm have a neutral pH (89). However, it is not known if such pH changes can alter the topology of mTMDs via changes to the protonation state of Asp, Glu, or histidine residues. A second important consideration is that the ER and PM are different both in terms of lipid composition and asymmetry. Thus, the ER is delineated by a symmetric membrane, whereas the PM exhibits asymmetry of multiple lipid species, including PS (4). We have shown recently that the topology of pHLIP is affected by the changes in symmetric lipid composition (28). Here, we show that even a small level of PS asymmetry in the bilayer impacts the location of pHLIP in the membrane. In future work, we are interested in determining if asymmetry changes to the ER and PM can trigger mTMD

topological changes, which could affect the folding and activity of membrane proteins in different cellular membranes.

SUPPORTING MATERIAL

Supporting Material can be found online at https://doi.org/10.1016/j.bpj.2019.03.003.

AUTHOR CONTRIBUTIONS

H.L.S. performed the research. H.L.S., F.A.H., and F.N.B. designed the research and analyzed the data. H.L.S., F.A.H., J.K., and F.N.B. wrote the manuscript.

ACKNOWLEDGMENTS

We thank Dr. Drew Marquardt for thoughtful discussions about determining the level of PS asymmetry and help with the nuclear magnetic resonance assays; Dr. Ilya Levental, Vanessa P. Nguyen, and Justin M. Westerfield for comments on the manuscript; and Forrest L. Davis for performing experiments.

This work was partially supported by grant R01GM120642 from the National Institutes of Health (F.N.B.), National Science Foundation grant number MCB-1817929 (F.A.H.), and by funds from the University of Tennessee Oak Ridge National Laboratory Joint Institute for Biological Sciences to F.N.B. Support was also received from the University of Tennessee Oak Ridge National Laboratory Science Alliance in the form of a Joint Directed Research and Development Award (to F.N.B.). aLUV preparation, GC/MS, and DLS measurements were supported by the Biophysical Characterization Laboratory suite of the Shull Wollan Center at Oak Ridge National Laboratory. J.K. is supported through the Scientific User Facilities Division of the Department of Energy Office of Science, sponsored by the Basic Energy Science Program, Department of Energy Office of Science, under contract number DEAC05-00OR22725.

REFERENCES

1. Bretscher, M. S. 1972. Asymmetrical lipid bilayer structure for biological membranes. *Nat. New Biol.* 236:11–12.
2. Verkleij, A. J., R. F. Zwaal, …, L. L. van Deenen. 1973. The asymmetric distribution of phospholipids in the human red cell membrane. A combined study using phospholipases and freeze-etch electron microscopy. *Biochim. Biophys. Acta.* 323:178–193.
3. Op den Kamp, J. A. 1979. Lipid asymmetry in membranes. *Annu. Rev. Biochem.* 48:47–71.
4. van Meer, G., D. R. Voelker, and G. W. Feigenson. 2008. Membrane lipids: where they are and how they behave. *Nat. Rev. Mol. Cell Biol.* 9:112–124.
5. Manno, S., Y. Takakuwa, and N. Mohandas. 2002. Identification of a functional role for lipid asymmetry in biological membranes: phosphatidylserine-skeletal protein interactions modulate membrane stability. *Proc. Natl. Acad. Sci. USA.* 99:1943–1948.
6. Seigneuret, M., and P. F. Devaux. 1984. ATP-dependent asymmetric distribution of spin-labeled phospholipids in the erythrocyte membrane: relation to shape changes. *Proc. Natl. Acad. Sci. USA.* 81:3751–3755.
7. Smith, B. D., and T. N. Lambert. 2003. Molecular ferries: membrane carriers that promote phospholipid flip-flop and chloride transport. *Chem. Commun. (Camb.).* 18:2261–2268.
8. Helvoort, A., A. J. Smith, …, G. v. Meer. 1996. MDR1 P-glycoprotein is a lipid translocase of broad specificity, while MDR3 P-glycoprotein specifically translocates phosphatidylcholine. *Cell.* 87:507–517.
9. van den Eijnde, S. M., L. Boshart, …, C. Vermeij-Keers. 1998. Cell surface exposure of phosphatidylserine during apoptosis is phylogenetically conserved. *Apoptosis.* 3:9–16.
10. Rousselet, A., C. Guthmann, …, P. F. Devaux. 1976. Study of the transverse diffusion of spin labeled phospholipids in biological membranes. I. Human red bloods cells. *Biochim. Biophys. Acta.* 426:357–371.
11. Caberoy, N. B., Y. Zhou, …, W. Li. 2009. Efficient identification of phosphatidylserine-binding proteins by ORF phage display. *Biochem. Biophys. Res. Commun.* 386:197–201.
12. Yeung, T., G. E. Gilbert, …, S. Grinstein. 2008. Membrane phosphatidylserine regulates surface charge and protein localization. *Science.* 319:210–213.
13. Zhao, J., Q. Zhou, …, P. J. Sims. 1998. Level of expression of phospholipid scramblase regulates induced movement of phosphatidylserine to the cell surface. *J. Biol. Chem.* 273:6603–6606.
14. Guidotti, G. 1972. Membrane proteins. *Annu. Rev. Biochem.* 41:731–752.
15. Dupuy, A. D., and D. M. Engelman. 2008. Protein area occupancy at the center of the red blood cell membrane. *Proc. Natl. Acad. Sci. USA.* 105:2848–2852.
16. Tourasse, N. J., and W.-H. Li. 2000. Selective constraints, amino acid composition, and the rate of protein evolution. *Mol. Biol. Evol.* 17:656–664.
17. Bañó-Polo, M., C. Baeza-Delgado, …, I. Mingarro. 2018. Transmembrane but not soluble helices fold inside the ribosome tunnel. *Nat. Commun.* 9:5246.
18. Scott, H. L., J. M. Westerfield, and F. N. Barrera. 2017. Determination of the membrane translocation pK of the pH-low insertion peptide. *Biophys. J.* 113:869–879.
19. Shu, N. S., M. S. Chung, …, W. Qiang. 2015. Residue-specific structures and membrane locations of pH-low insertion peptide by solid-state nuclear magnetic resonance. *Nat. Commun.* 6:7787.
20. Cymer, F., G. von Heijne, and S. H. White. 2015. Mechanisms of integral membrane protein insertion and folding. *J. Mol. Biol.* 427:999–1022.
21. Vitrac, H., D. M. MacLean, …, W. Dowhan. 2015. Dynamic membrane protein topological switching upon changes in phospholipid environment. *Proc. Natl. Acad. Sci. USA.* 112:13874–13879.
22. Cheng, H. T., Megha, and E. London. 2009. Preparation and properties of asymmetric vesicles that mimic cell membranes: effect upon lipid raft formation and transmembrane helix orientation. *J. Biol. Chem.* 284:6079–6092.
23. Devaux, P. F., and R. Morris. 2004. Transmembrane asymmetry and lateral domains in biological membranes. *Traffic.* 5:241–246.
24. Reshetnyak, Y. K., M. Segala, …, D. M. Engelman. 2007. A monomeric membrane peptide that lives in three worlds: in solution, attached to, and inserted across lipid bilayers. *Biophys. J.* 93:2363–2372.
25. Deacon, J. C., D. M. Engelman, and F. N. Barrera. 2015. Targeting acidity in diseased tissues: mechanism and applications of the membrane-inserting peptide, pHLIP. *Arch. Biochem. Biophys.* 565:40–48.
26. Fattal, E., S. Nir, …, F. C. Szoka, Jr. 1994. Pore-forming peptides induce rapid phospholipid flip-flop in membranes. *Biochemistry.* 33:6721–6731.
27. Hunt, J. F., P. Rath, …, D. M. Engelman. 1997. Spontaneous, pH-dependent membrane insertion of a transbilayer alpha-helix. *Biochemistry.* 36:15177–15192.
28. Scott, H. L., V. P. Nguyen, …, F. N. Barrera. 2015. The negative charge of the membrane has opposite effects on the membrane entry and exit of pH-low insertion peptide. *Biochemistry.* 54:1709–1712.
29. Heberle, F. A., D. Marquardt, …, G. Pabst. 2016. Subnanometer structure of an asymmetric model membrane: interleaflet coupling influences domain properties. *Langmuir.* 32:5195–5200.

30. Doktorova, M., F. A. Heberle, …, D. Marquardt. 2018. Preparation of asymmetric phospholipid vesicles for use as cell membrane models. *Nat. Protoc.* 13:2086–2101.

31. Kingsley, P. B., and G. W. Feigenson. 1979. The synthesis of a perdeuterated phospholipid: 1,2-dimyristoyl-*sn*-glycero-3-phosphocholine-d_{72}. *Chem. Phys. Lipids.* 24:135–147.

32. Weerakkody, D., A. Moshnikova, …, Y. K. Reshetnyak. 2013. Family of pH (low) insertion peptides for tumor targeting. *Proc. Natl. Acad. Sci. USA.* 110:5834–5839.

33. White, S. H., and W. C. Wimley. 1999. Membrane protein folding and stability: physical principles. *Annu. Rev. Biophys. Biomol. Struct.* 28:319–365.

34. Butt, H. J., K. Graf, and M. Kappl. 2006. Physics and Chemistry of Interfaces. Wiley-VCH, Berlin, Germany.

35. Pan, J., X. Cheng, …, J. Katsaras. 2014. The molecular structure of a phosphatidylserine bilayer determined by scattering and molecular dynamics simulations. *Soft Matter.* 10:3716–3725.

36. Barrera, F. N., D. Weerakkody, …, D. M. Engelman. 2011. Roles of carboxyl groups in the transmembrane insertion of peptides. *J. Mol. Biol.* 413:359–371.

37. Barrera, F. N., M. T. Garzón, …, J. L. Neira. 2002. Equilibrium unfolding of the C-terminal SAM domain of p73. *Biochemistry.* 41:5743–5753.

38. Royer, C. A., and S. F. Scarlata. 2008. Fluorescence approaches to quantifying biomolecular interactions. *Methods Enzymol.* 450:79–106.

39. Ladokhin, A. S., S. Jayasinghe, and S. H. White. 2000. How to measure and analyze tryptophan fluorescence in membranes properly, and why bother? *Anal. Biochem.* 285:235–245.

40. Kelly, S. M., T. J. Jess, and N. C. Price. 2005. How to study proteins by circular dichroism. *Biochim. Biophys. Acta.* 1751:119–139.

41. Marquardt, D., B. Geier, and G. Pabst. 2015. Asymmetric lipid membranes: towards more realistic model systems. *Membranes (Basel).* 5:180–196.

42. St. Clair, J. R., Q. Wang, …, E. London. 2017. Preparation and Physical Properties of Asymmetric Model Membrane Vesicles. *In* The Biophysics of Cell Membranes R. Epand and J. M. Ruysschaert, eds. . Springer, pp. 1–27.

43. Cheng, H. T., and E. London. 2011. Preparation and properties of asymmetric large unilamellar vesicles: interleaflet coupling in asymmetric vesicles is dependent on temperature but not curvature. *Biophys. J.* 100:2671–2678.

44. Tait, J. F., and D. Gibson. 1992. Phospholipid binding of annexin V: effects of calcium and membrane phosphatidylserine content. *Arch. Biochem. Biophys.* 298:187–191.

45. Koopman, G., C. P. Reutelingsperger, …, M. H. van Oers. 1994. Annexin V for flow cytometric detection of phosphatidylserine expression on B cells undergoing apoptosis. *Blood.* 84:1415–1420.

46. Liu, J., and J. C. Conboy. 2004. Direct measurement of the transbilayer movement of phospholipids by sum-frequency vibrational spectroscopy. *J. Am. Chem. Soc.* 126:8376–8377.

47. Marquardt, D., F. A. Heberle, …, G. Pabst. 2017. ^{1}H NMR shows slow phospholipid flip-flop in gel and fluid bilayers. *Langmuir.* 33:3731–3741.

48. Kaihara, M., H. Nakao, …, M. Nakano. 2013. Control of phospholipid flip-flop by transmembrane peptides. *Chem. Phys.* 419:78–83.

49. Kol, M. A., A. N. van Laak, …, B. de Kruijff. 2003. Phospholipid flop induced by transmembrane peptides in model membranes is modulated by lipid composition. *Biochemistry.* 42:231–237.

50. Kol, M. A., A. I. de Kroon, …, B. de Kruijff. 2001. Membrane-spanning peptides induce phospholipid flop: a model for phospholipid translocation across the inner membrane of *E. coli*. *Biochemistry.* 40:10500–10506.

51. Karabadzhak, A. G., D. Weerakkody, …, Y. K. Reshetnyak. 2012. Modulation of the pHLIP transmembrane helix insertion pathway. *Biophys. J.* 102:1846–1855.

52. Andreev, O. A., A. G. Karabadzhak, …, Y. K. Reshetnyak. 2010. pH (low) insertion peptide (pHLIP) inserts across a lipid bilayer as a helix and exits by a different path. *Proc. Natl. Acad. Sci. USA.* 107:4081–4086.

53. Hanz, S. Z., N. S. Shu, …, W. Qiang. 2016. Protonation-driven membrane insertion of a pH-low insertion peptide. *Angew. Chem. Int.Engl.* 55:12376–12381.

54. Barrera, F. N., J. Fendos, and D. M. Engelman. 2012. Membrane physical properties influence transmembrane helix formation. *Proc. Natl. Acad. Sci. USA.* 109:14422–14427.

55. Johnson, A. E. 2005. Fluorescence approaches for determining protein conformations, interactions and mechanisms at membranes. *Traffic.* 6:1078–1092.

56. Chattopadhyay, A. 1990. Chemistry and biology of N-(7-nitrobenz-2-oxa-1,3-diazol-4-yl)-labeled lipids: fluorescent probes of biological and model membranes. *Chem. Phys. Lipids.* 53:1–15.

57. Ladokhin, A. S. 2013. pH-triggered conformational switching along the membrane insertion pathway of the diphtheria toxin T-domain. *Toxins (Basel).* 5:1362–1380.

58. Kyrychenko, A., Y. O. Posokhov, …, A. S. Ladokhin. 2009. Kinetic intermediate reveals staggered pH-dependent transitions along the membrane insertion pathway of the diphtheria toxin T-domain. *Biochemistry.* 48:7584–7594.

59. Bergen, J. M., E. J. Kwon, …, S. H. Pun. 2008. Application of an environmentally sensitive fluorophore for rapid analysis of the binding and internalization efficiency of gene carriers. *Bioconjug. Chem.* 19:377–384.

60. Popot, J.-L., and D. M. Engelman. 1990. Membrane protein folding and oligomerization: the two-stage model. *Biochemistry.* 29:4031–4037.

61. Rosing, J., E. M. Bevers, …, R. F. Zwaal. 1985. Impaired factor X and prothrombin activation associated with decreased phospholipid exposure in platelets from a patient with a bleeding disorder. *Blood.* 65:1557–1561.

62. Bozelli, J. C., Jr., Y. H. Hou, and R. M. Epand. 2017. Thermodynamics of methyl-β-cyclodextrin-induced lipid vesicle solubilization: effect of lipid headgroup and backbone. *Langmuir.* 33:13882–13891.

63. Huang, Z., and E. London. 2013. Effect of cyclodextrin and membrane lipid structure upon cyclodextrin-lipid interaction. *Langmuir.* 29:14631–14638.

64. Lin, Q., and E. London. 2014. Preparation of artificial plasma membrane mimicking vesicles with lipid asymmetry. *PLoS One.* 9:e87903.

65. Chen, H., S. S. Ahsan, …, W. W. Webb. 2010. Mechanisms of quenching of Alexa fluorophores by natural amino acids. *J. Am. Chem. Soc.* 132:7244–7245.

66. Reshetnyak, Y. K., O. A. Andreev, …, D. M. Engelman. 2008. Energetics of peptide (pHLIP) binding to and folding across a lipid bilayer membrane. *Proc. Natl. Acad. Sci. USA.* 105:15340–15345.

67. Kyrychenko, A., V. Vasquez-Montes, …, A. S. Ladokhin. 2015. Lipid headgroups modulate membrane insertion of pHLIP peptide. *Biophys. J.* 108:791–794.

68. Tsui, F. C., D. M. Ojcius, and W. L. Hubbell. 1986. The intrinsic pKa values for phosphatidylserine and phosphatidylethanolamine in phosphatidylcholine host bilayers. *Biophys. J.* 49:459–468.

69. Marsh, D. 2013. Handbook of Lipid Bilayers. CRC Press, Boca Raton.

70. Gurtovenko, A. A., and I. Vattulainen. 2008. Membrane potential and electrostatics of phospholipid bilayers with asymmetric transmembrane distribution of anionic lipids. *J. Phys. Chem. B.* 112:4629–4634.

71. Wang, L. 2012. Measurements and implications of the membrane dipole potential. *Annu. Rev. Biochem.* 81:615–635.

72. Hall, J. E., and R. Latorre. 1976. Nonactin-K+ complex as a probe for membrane asymmetry. *Biophys. J.* 16:99–103.

73. Gurtovenko, A. A., and I. Vattulainen. 2007. Lipid transmembrane asymmetry and intrinsic membrane potential: two sides of the same coin. *J. Am. Chem. Soc.* 129:5358–5359.

74. McLaughlin, S. 1989. The electrostatic properties of membranes. *Annu. Rev. Biophys. Biophys. Chem.* 18:113–136.

75. Pace, C. N., G. R. Grimsley, and J. M. Scholtz. 2009. Protein ionizable groups: pK values and their contribution to protein stability and solubility. *J. Biol. Chem.* 284:13285–13289.

76. Xu, C., and L. M. Loew. 2003. The effect of asymmetric surface potentials on the intramembrane electric field measured with voltage-sensitive dyes. *Biophys. J.* 84:2768–2780.

77. Taylor, G., M. A. Nguyen, …, S. A. Sarles. 2019. Electrophysiological interrogation of asymmetric droplet interface bilayers reveals surface-bound alamethicin induces lipid flip-flop. *Biochim. Biophys. Acta. Biomembr.* 1861:335–343.

78. Popot, J. L., and D. M. Engelman. 2000. Helical membrane protein folding, stability, and evolution. *Annu. Rev. Biochem.* 69:881–922.

79. Mitra, K., T. A. Steitz, and D. M. Engelman. 2002. Rational design of 'water-soluble' bacteriorhodopsin variants. *Protein Eng.* 15:485–492.

80. Murtazina, R., B. J. Booth, …, L. Fliegel. 2001. Functional analysis of polar amino-acid residues in membrane associated regions of the NHE1 isoform of the mammalian Na+/H+ exchanger. *Eur. J. Biochem.* 268:4674–4685.

81. Zhao, G., and E. London. 2006. An amino acid "transmembrane tendency" scale that approaches the theoretical limit to accuracy for prediction of transmembrane helices: relationship to biological hydrophobicity. *Protein Sci.* 15:1987–2001.

82. Hedin, L. E., K. Ojemalm, …, A. Elofsson. 2010. Membrane insertion of marginally hydrophobic transmembrane helices depends on sequence context. *J. Mol. Biol.* 396:221–229.

83. Krishnakumar, S. S., and E. London. 2007. The control of transmembrane helix transverse position in membranes by hydrophilic residues. *J. Mol. Biol.* 374:1251–1269.

84. Bogdanov, M., W. Dowhan, and H. Vitrac. 2014. Lipids and topological rules governing membrane protein assembly. *Biochim. Biophys. Acta.* 1843:1475–1488.

85. London, E., and K. Shahidullah. 2009. Transmembrane vs. non-transmembrane hydrophobic helix topography in model and natural membranes. *Curr. Opin. Struct. Biol.* 19:464–472.

86. Öjemalm, K., H. R. Watson, …, S. High. 2013. Positional editing of transmembrane domains during ion channel assembly. *J. Cell Sci.* 126:464–472.

87. Lambert, C., S. Mann, and R. Prange. 2004. Assessment of determinants affecting the dual topology of hepadnaviral large envelope proteins. *J. Gen. Virol.* 85:1221–1225.

88. Lu, Y., I. R. Turnbull, …, W. R. Skach. 2000. Reorientation of aquaporin-1 topology during maturation in the endoplasmic reticulum. *Mol. Biol. Cell.* 11:2973–2985.

89. Rivinoja, A., F. M. Pujol, …, S. Kellokumpu. 2012. Golgi pH, its regulation and roles in human disease. *Ann. Med.* 44:542–554.